

Supporting Information

Multilayered Perovskite Materials Based on Polymeric-Ammonium Cations for Stable and Large-Area Solar Cell

Kai Yao, Xiaofeng Wang, Yun-xiang Xu, Fan Li, Lang Zhou

Experimental Section

Materials: All the chemicals were used as received, including PbI₂ (99%, Sigma–Aldrich), MAI (99%, Sigma–Aldrich), hydroiodic acid (57 wt% in water with 1.5% hypophosphorous acid, Alfa Aesar) and polyethylenimine, ethylenediamine branched (PEI, M_w ~ 800, Aldrich). Polymeric ammonium (PEI·HI) was synthesized as our previous work^[30]. 2D (PEI)₂(MA)_{n-1}Pb_nI_{3n+1} (*n* = 3, 5, 7) family of perovskite compounds were synthesized from a stoichiometric reaction between PbI₂, MAI, and n-butylamine (BA). Taking (PEI)₂(MA)₂Pb₃I₁₀ for example, solid PEI·HI (0.0011 mmol), MAI (0.010 mmol), and PbI₂ (0.015 mmol) were dissolved in 10mL γ-Butyrolactone (GBL) at 70°C. The stirring was then discontinued, and the solution was left to cool to room temperature during which time deep-red rectangular-shaped plates started to crystallize. The crystals were isolated by filtration and then dried under reduced pressure.

Device Fabrication: ITO (15 ohm/sq) on glass were cleaned sequentially with detergent and deionized water, acetone, and isopropanol under sonication for 10 min. Commercial aqueous dispersion of PEDOT:PSS (Clevios PVP Al 4083) was spin-coated (4k rpm) on pre-cleaned and dry ITO substrate. For MAPbI₃ and 2D perovskite films deposition, the 1.0 M Pb²⁺ perovskite precursors in DMF were spin-coated at 3000 rpm for 40 s. While for modified method for MAPbI₃ perovskite layer deposition was carried out using solvent-engineering: first, the 1.0 M DMF solution of PbI₂/MAI mixture was spread onto the substrate; then, the spin-coater was started at a rotation speed of 1000 rpm for 10

seconds and 5000 rpm for another 30 seconds. 200 μ l toluene was drop-casted quickly 10 seconds after the 5000 rpm spin-coating started. The MAPbI₃ perovskite films were then heated at 100 °C on a hotplate for 10 min. Afterward, the PC₆₁BM (20 mg/mL in chlorobenzene) was then sequentially deposited by spin coating at 1.2 k rpm for 60 s. LiF interlayer and Ag electrode were thermally evaporated on top of the film under high vacuum ($<2 \times 10^{-6}$ Torr) with the thickness of 1 nm and 200 nm, respectively, through a shadow mask of various area (0.04, 0.82 or 2.32 cm²).

Characterizations: SEM images were obtained by using a JSM-6500F field-emission scanning electron microscope. The UPS measurements were performed in a Kratos Ultra Spectrometer (AXIS-ULTRA DLD-600W) using monochromatized HeI (21.2 eV for UPS) discharge lamp. The IPES spectra were recorded using a custom-made spectrometer, composed of a commercial Kimball Physics ELG-2 electron gun and a band pass photon detector. The photon detector worked in the isochromatic mode centered at a fixed energy of 9.8 eV. The current-voltage characteristics were measured using a black metal mask with an aperture area of 0.04, 0.82 or 2.32 cm² under standard air mass 1.5 sunlight (300 W xenon arc solar simulator). The illumination intensity of the light source was accurately calibrated employing a standard Si photodiode detector equipped with a KG-5 filter, which can be traced back to the standard cell of the National Renewable Energy Laboratory (NREL). The EQE spectra performed here were obtained from an IPCE setup consisting of a Xenon lamp (Oriel, 450 W) as the light source, a monochromator, a chopper with a frequency of 100Hz, a lock-in amplifier, and a Si-based diode for calibration. The calculated J_{sc} values obtained by integrating the EQE spectrum under the AM 1.5G illumination condition agreed well with the measured J_{sc}

value from J - V characteristics and the differences were within 3%. The time-resolved photoluminescence characterizations were done on an Edinburg FLS 920 (Edinburg90 Co. LTD).

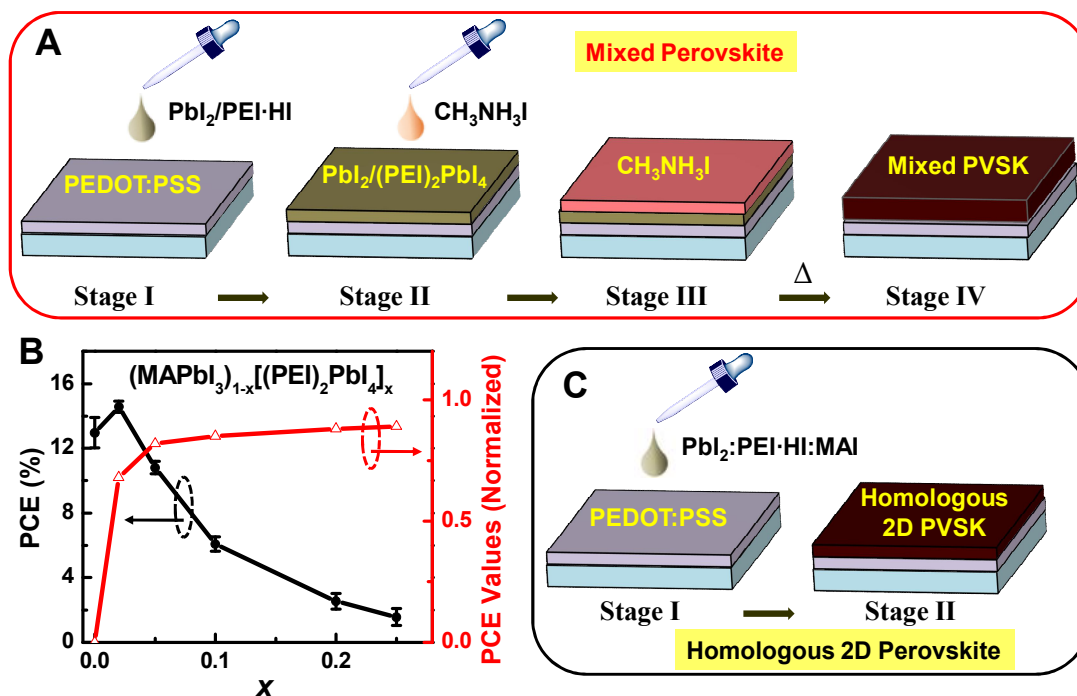


Figure S1. A) Schematic of mixed perovskite $(\text{MAPbI}_3)_{1-x}[(\text{PEI})_2\text{PbI}_4]_x$ processed from two-step method. B) Left: Initial PCE values for cells using $(\text{MAPbI}_3)_{1-x}[(\text{PEI})_2\text{PbI}_4]_x$ materials; Right: Moisture stability of a photovoltaic device fabricated from perovskite films with different compositions after storing for a month. C) Schematic of 2D homologous perovskite $(\text{PEI})_2(\text{MA})_{n-1}\text{Pb}_n\text{I}_{3n+1}$ processed from one-step method.

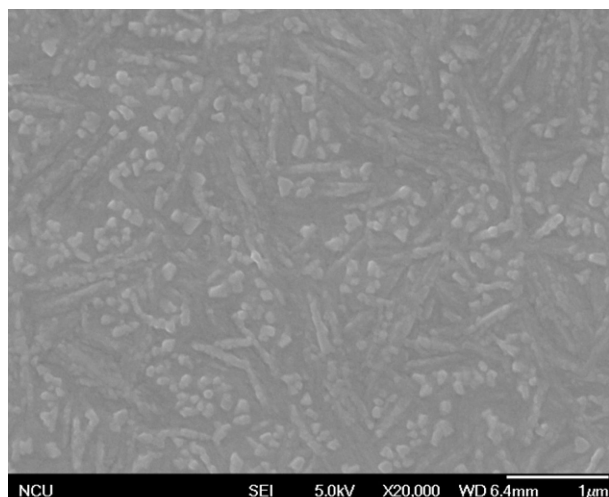


Figure S2. The surface-view SEM images of the mixed perovskite $(\text{MAPbI}_3)_{1-x}[(\text{PEI})_2\text{PbI}_4]_x$ film with the containing of layered perovskite about (x value) 20%. The large phase-separation of the films indicated the severe carrier recombination in the bulk.

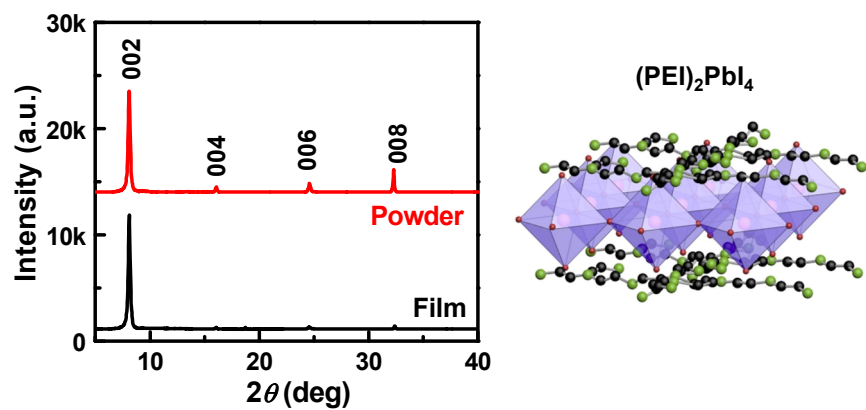


Figure S3. XRD pattern of thin films and bulk materials of 2D perovskites $(\text{PEI})_2\text{PbI}_4$, with the schematic structure.

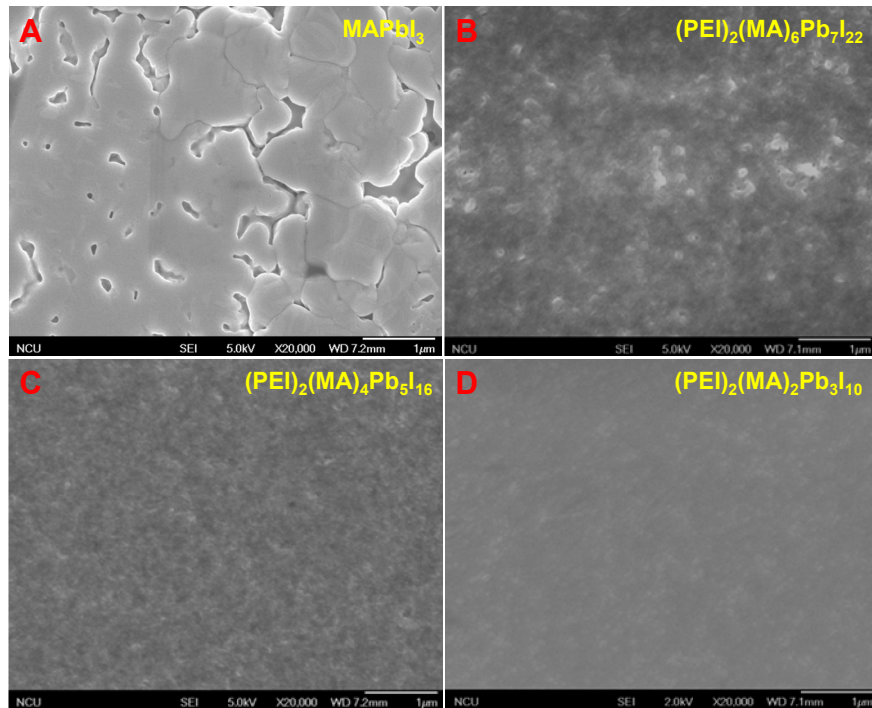


Figure S4. Top surface SEM images of MAPbI_3 and $(\text{PEI})_2(\text{MA})_{n-1}\text{Pb}_n\text{I}_{3n+1}$ films.

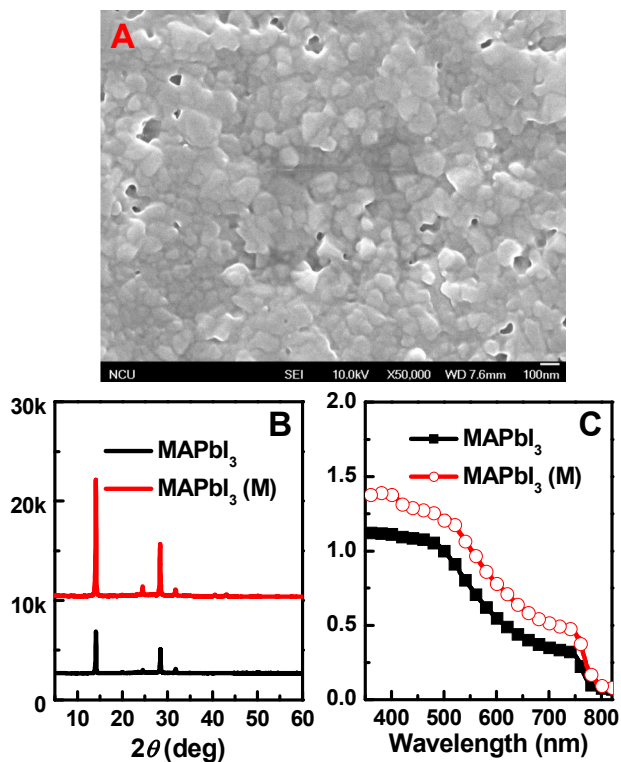


Figure S5. The surface-view SEM images (A), XRD patterns (B) and absorption spectra (C) of the MAPbI₃ (M) film prepared by solution-engineering approach. The increased light absorption and enhanced reflection intensities confirmed the formation of highly crystallized MAPbI₃ films under the modified methods.

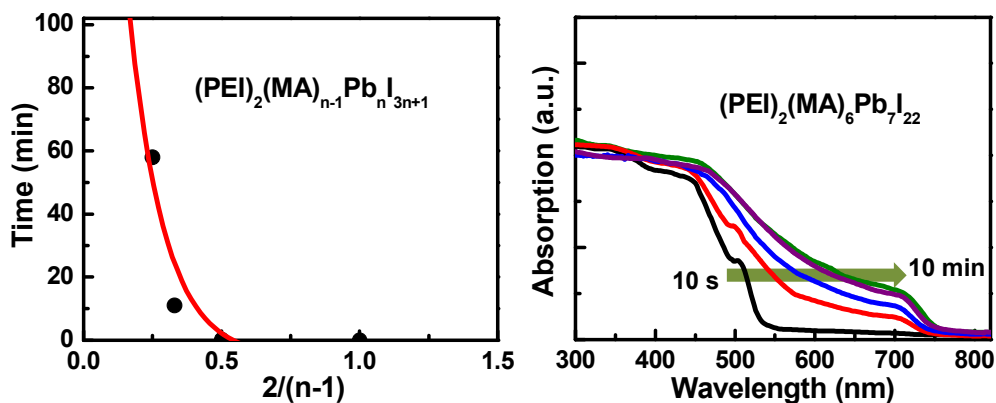


Figure S6. (A) The time for multilayered structure formation of different (PEI)₂(MA)_{n-1}Pb_nI_{3n+1} ($n = 3, 5, 7$) perovskite compounds, based on the UV-vis absorption data; (B) The absorption of the (PEI)₂(MA)₆Pb₇I₂₂ films with various placement time (10 s, 60 s, 4 min, 8 min and 10 min). From absorption spectra, both PbI₂ and perovskite coexist in the film in initial stage.

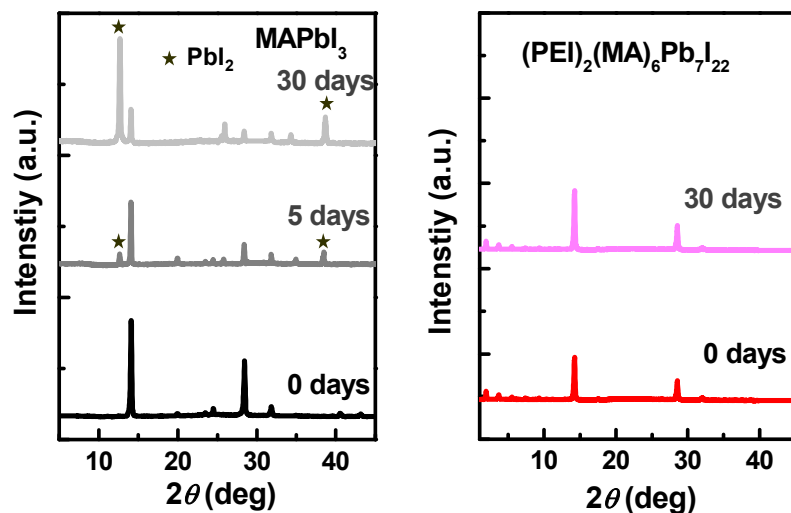


Figure S7. XRD patterns of films of MAPbI₃ and (PEI)₂(MA)₆Pb₇I₂₂ exposed to 50% relative humidity. Asterisks denote the major reflections from PbI₂.

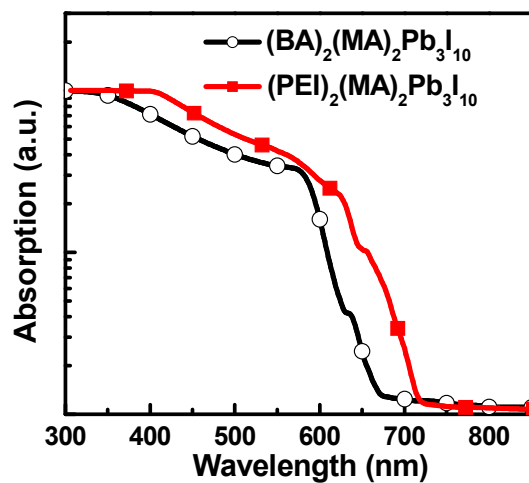


Figure S8. UV-visible absorbance spectrum of (PEI)₂(MA)₂Pb₃I₁₀ and (BA)₂(MA)₂Pb₃I₁₀. The change of the band gap indicated the interaction of between the organic and inorganic components.

Table S1 Time resolved photoluminescence characterization of the various perovskite films.^{1, 2}

Compounds	Fraction 1	τ_1 (ns)	Fraction 2	τ_2 (ns)
MAPbI ₃	79%	8.04	21%	81.47
(PEI) ₂ (MA) ₆ Pb ₇ I ₂₂	84%	5.72	16%	25.24
(BA) ₂ (MA) ₆ Pb ₇ I ₂₂	100%	4.11	-	-

Note 1: We prepared the perovskite layers with sealing of a 50-nm-thick poly(methylmethacrylate) (PMMA) layer.

Note 2: The lifetime was obtained by fitting the PL measured from perovskite films with a bi-exponential decay function of the form:

$$I(t) = A_1 \exp\left(-\frac{t}{\tau_1}\right) + A_2 \exp\left(-\frac{t}{\tau_2}\right)$$

Note 3: The two fractions in the PL decay of (BA)₂(MA)₆Pb₇I₂₂ films were found in the same, which demonstrated the mono-exponential decay.

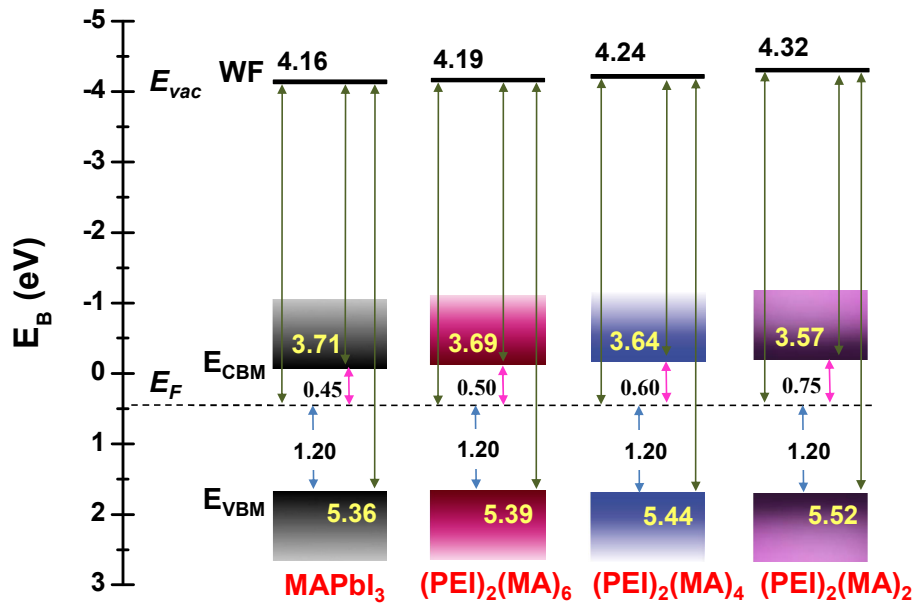


Figure S9. Experimentally determined energy level diagrams of MAPbI₃ and (PEI)₂(MA)_{n-1}Pb_nI_{3n+1} ($n = 3, 5, 7$) films from UPS and IPES spectra. Each diagram provides the Fermi level position, work function, conduction band minimum (CBM) and valence band maximum (VBM).

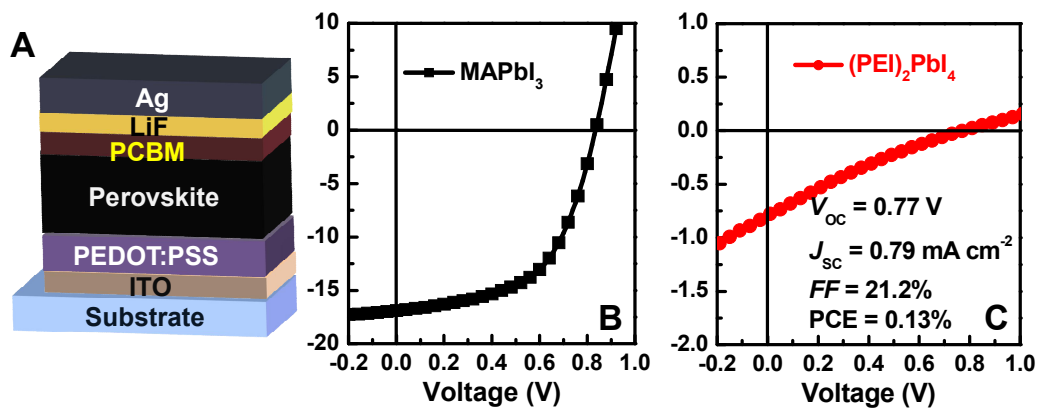


Figure S10. (A) Diagram of the cell configuration; J - V curves of MAPbI_3 (B) and $(\text{PEI})_2\text{PbI}_4$ (C) solar cells deposited from conventional one-step spin-coating process.

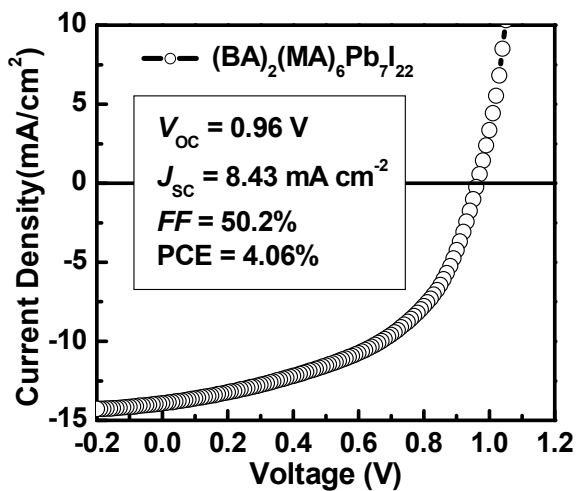


Figure S11. The characterization of photovoltaic performance: J - V curves of $(\text{BA})_2(\text{MA})_6\text{Pb}_7\text{I}_{22}$ -based devices.

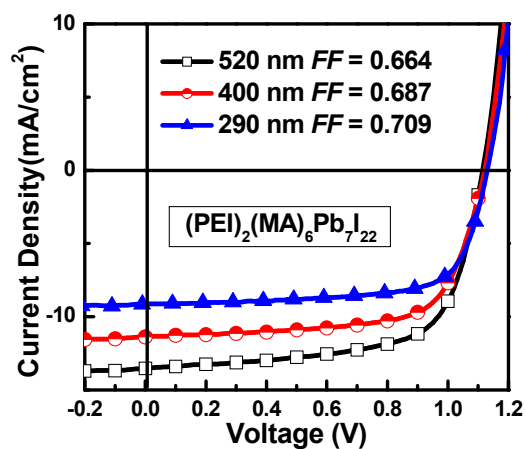


Figure S12. J - V curves of $(\text{PEI})_2(\text{MA})_6\text{Pb}_7\text{I}_{22}$ -based devices with various active layer thickness.

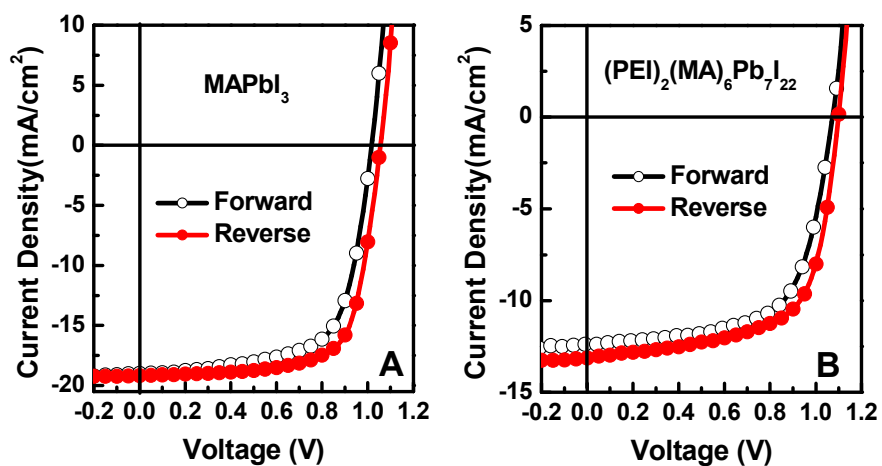


Figure S13. J - V curves of forward and reverse bias sweep for the solar cell using the MAPbI_3 (M) and $(\text{PEI})_2(\text{MA})_6\text{Pb}_7\text{I}_{22}$ perovskite active layer, step width = 50 mV and delay time = 5000 ms.

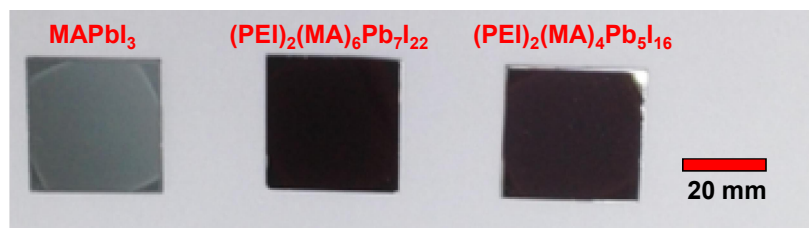


Figure S14. Digital photograph of MAPbI₃ and (PEI)₂(MA)_{n-1}Pb_nI_{3n+1} ($n = 5, 7$) films in relative large area (3.5 cm × 3.5 cm).

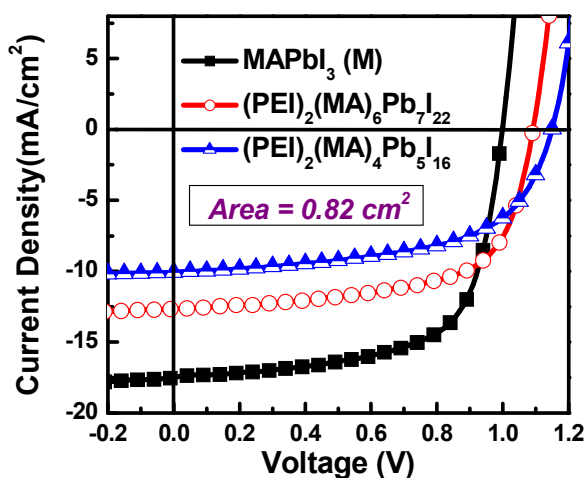


Figure S15. J - V curve for the (PEI)₂(MA)_{n-1}Pb_nI_{3n+1} perovskites and MAPbI₃ (M) based devices in aperture area of 0.82 cm².

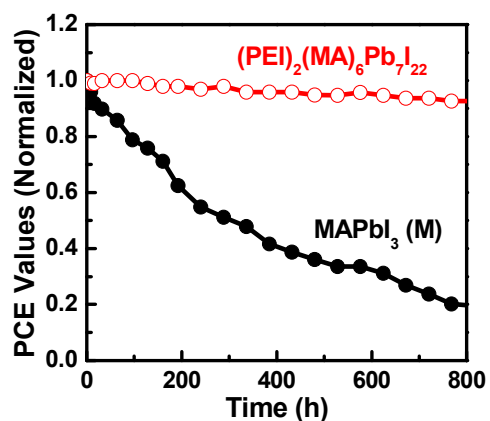


Figure S16. Stability of MAPbI₃ and (PEI)₂(MA)₆Pb₇I₂₂ cells (unsealed) kept in the dark.

Table S2 Performance of perovskite devices under AM 1.5G illumination (100 mW cm⁻²) with small-size cells (0.82 cm²). The fabrication procedure was similar for all devices in optimized condition.

Device	J_{sc} (mA cm ⁻²)	V_{oc} (V)	FF	PCE (%) ^a
MAPbI ₃ (M)	17.51 ± 0.75	1.00 ± 0.04	0.66 ± 0.03	11.76 ± 0.71 (12.98)
(PEI) ₂ (MA) ₆ Pb ₇ I ₂₂	12.67 ± 0.50	1.09 ± 0.02	0.64 ± 0.02	8.87 ± 0.45 (9.49)
(PEI) ₂ (MA) ₄ Pb ₅ I ₁₆	10.07 ± 0.42	1.15 ± 0.01	0.58 ± 0.01	6.77 ± 0.41 (7.16)